

Article

# First-Stage Dynamics of the Immune System and Cancer

Roberto Herrero <sup>\*,†</sup> , Joan Nieves <sup>†</sup>  and Augusto Gonzalez <sup>†</sup> 

Institute of Cybernetics, Mathematics and Physics, Havana 10400, Cuba; joan.nieves@icimaf.cu (J.N.); agonzale@icimaf.cu (A.G.)

\* Correspondence: rohepe@icimaf.cu

† These authors contributed equally to this work.

**Abstract:** The innate immune system is the first line of defense against pathogens. Its composition includes barriers, mucus, and other substances as well as phagocytic and other cells. The purpose of the present paper is to compare tissues with regard to their immune response to infections and to cancer. Simple ideas and the qualitative theory of differential equations are used along with general principles such as the minimization of the pathogen load and economy of resources. In the simplest linear model, the annihilation rate of pathogens in any tissue should be greater than the pathogen's average replication rate. When nonlinearities are added, a stability condition emerges, which relates the strength of regular threats, barrier height, and annihilation rate. The stability condition allows for a comparison of immunity in different tissues. On the other hand, in cancer immunity, the linear model leads to an expression for the lifetime risk, which accounts for both the effects of carcinogens (endogenous or external) and the immune response. The way the tissue responds to an infection shows a correlation with the way it responds to cancer. The results of this paper are formulated in the form of precise statements in such a way that they could be checked by present-day quantitative immunology.

**Keywords:** immune system; dynamics; infectious process; cancer



**Citation:** Herrero, R.; Nieves, J.; Gonzalez, A. First-Stage Dynamics of the Immune System and Cancer. *AppliedMath* **2023**, *3*, 1034–1044. <https://doi.org/10.3390/appliedmath3040052>

Academic Editor: Thomas Woolley

Received: 27 September 2023

Revised: 13 November 2023

Accepted: 28 November 2023

Published: 12 December 2023



**Copyright:** © 2023 by the authors. Licensee MDPI, Basel, Switzerland. This article is an open access article distributed under the terms and conditions of the Creative Commons Attribution (CC BY) license (<https://creativecommons.org/licenses/by/4.0/>).

## 1. Introduction

Human immunity is, as are practically all physical aspects of life, a control process. Our body senses the number of pathogens in a tissue and a response is generated, which reduces the pathogen load.

The vertebrate's immune system has evolved over millions of years to protect the host from infection through a multilayered defense strategy, compressing a variety of sensors, signals, and effectors at the cellular level [1]. This includes the innate and adaptive arms of immunity, which work cooperatively to recognize, respond to, and remember pathogens.

The innate immune system provides rapid first-line protection against infection in a nonspecific manner. Its components include physical and chemical barriers, phagocytic cells (neutrophils and monocytes/macrophages), natural killer (NK) cells, the complement system, and inflammatory signaling molecules called cytokines. Innate immune defenses identify pathogens through pattern-recognition receptors (PRRs) [2] that bind conserved molecular patterns on microbes, known as pathogen-associated molecular patterns (PAMPs). Innate immunity is also known to play an important role in antitumor responses by detecting tumors, activating adaptive immunity, and exerting direct effector functions on emerging cancer cells [3].

The mathematical modeling of such a complex system is, of course, a very difficult task. Excellent reviews can be found on both modeling infections [4–7] and cancer [8–11], in which a historical perspective is offered and details of the models are discussed. With regard to our paper, we find similarities with the works by Prof. Marchuk's group [12,13]. A very nice resume of that work is presented in Ref. [14]. We, as in [14], use differential

equations to model the system and emphasize the qualitative aspects. However, there are also essential differences.

First, in our paper, we use simple models and very general principles, such as minimization of the pathogen load and economy of resources, in order to put bounds on the constants entering the model or to obtain inequalities for the stability of a tissue. These inequalities allow a direct comparison of the immune response in different tissues. To the best of our knowledge, there are no similar results in the literature. Even in a reference like [15], where different tissues are studied, there is no aim at performing such a comparison.

Second, we use a simple linear model for the very early stages of carcinogenesis in order to obtain an expression for the risk of cancer in a tissue. This expression is consistent with the data on cancer risk in different tissues [16] and with a model of random jumps in the gene-expression space [17]. On the other hand, an interesting correlation is suggested between the way a tissue responds to an infection and its response to cancer. To the best of our knowledge, these are also new results.

The results of our paper are presented in the form of precise statements. The idea is to motivate experimental immunologists, who could attempt a direct check.

The plan of this paper is as follows. The linear model is presented in Section 2.1. Even from this simplest model, a statement is derived. Nonlinearities are introduced in Section 2.2. Consequences of the nonlinear model are discussed in the subsequent sections. In particular, Section 2.4 formulates a stability condition relating the regular pathogen threat with the immune barrier and the pathogen annihilation rate with the tissue. The stability condition allows for a direct comparison of different tissues with regard to their immune responses. Immunity to cancer and its correlation with the immune response against an infection is discussed in Section 2.8. Finally, in Section 3, we present the discussion and some possible future directions of work.

## 2. Results

### 2.1. Linear Model

Let us consider, for example, a very small intensity threat to a given tissue in an adult individual. The resident cells of the immune system will trigger a response to clear the infection. These are, basically, resident cells of the innate system [18]. The simplest available model for the response is a linear one:

$$\frac{dP}{d\tau} = \alpha_t f_t + aP - b_t P, \quad (1)$$

in which the response is proportional to the threat.  $\tau$  is time;  $P$  is the number of pathogens (in some units); and  $a$  is its rate of growth, typically  $\sim 1/\text{hour}$  for bacteria [19]. A freely evolving group of a few streptococci, for example, would lead, in around 40 h, to a colony greater than the number of cells in the lungs.

The coefficient  $b_t$ , on the other hand, is the tissue-annihilation rate of pathogens which, for consistency, should be greater than  $a$  so that small threats do not transform into acute health problems in the short term. This condition requires enough number of resident immune cells in the tissue. This statement may be explicitly formulated and experimentally checked:

**Statement 1.** *In any tissue, the annihilation rate of pathogens, due to the resident immune cells, is greater than the average multiplication rate of pathogens.*

Finally,  $\alpha_t f_t$  is the rate of entrance of pathogens into the tissue. The constant  $\alpha_t < 1$  will model barrier or mucosal immunity; that is, the flow of pathogens,  $f_t$ , is partially trapped and cleared by the barrier or mucosa (or both).

According to Equation (1) and under the assumption that Statement 1 holds, a finite load of pathogens is always annihilated, irrespective of the total number. This unrealistic situation is corrected in nonlinear models, characteristic of self-regulated systems.

### 2.2. Nonlinear Model

In a real situation, neither the pathogen load nor the immune response can grow without limits. A nonlinear model prevents this unrealistic situation from taking place. For low pathogen loads (low  $P$ ), we should recover the linear regime, as before. We use a modification of Model 5 of Ref. [20] in order to take into account nonlinearities:

$$\frac{dP}{d\tau} = \alpha_t f_t + aP \left( 1 - \frac{P}{P_s} \right) - \frac{b_t P}{1 + c_\infty P}. \tag{2}$$

The  $a$  parameter, which has roughly the same meaning as in Equation (1), equals  $0.6 \text{ h}^{-1}$ . The added nonlinearity limits the increase in  $P$  to values below  $P_s = 20$ , a conventional parameter indicating sepsis. The authors of paper [20] use an average value of the annihilation rate,  $b_t$ , for the body of  $1.5 \text{ h}^{-1}$ , a value satisfying the requirement  $b > a$ , mentioned in the previous paragraph. The parameter  $c_\infty = 5$  also limits the immune response for high values of  $P$ .

The main deficiency of Equation (2) is the lack of a term modeling the recruitment of other immune cells. However, even from this simple model, we can obtain important properties with the help of the qualitative theory of differential equations [21].

### 2.3. Reference Value for the Number of Pathogens

As will become clear below, Equation (2) has three fixed points:  $P = 0$  (healthy tissue);  $P_s = 20$  (sepsis); and  $P = P_c$ , which is an unstable fixed point dividing healthy from septic conditions. We draw in Figure 1 the r.h.s. of Equation (2) for  $f_t = 0$ , which shows two of the fixed points:  $P = 0$  and  $P = P_c$ . If, in the time evolution according to Equation (2),  $P$  reaches values greater than  $P_c$ , then the outcome will be a state with  $P$  close to the third fixed point,  $P_s$ , not seen in the figure.

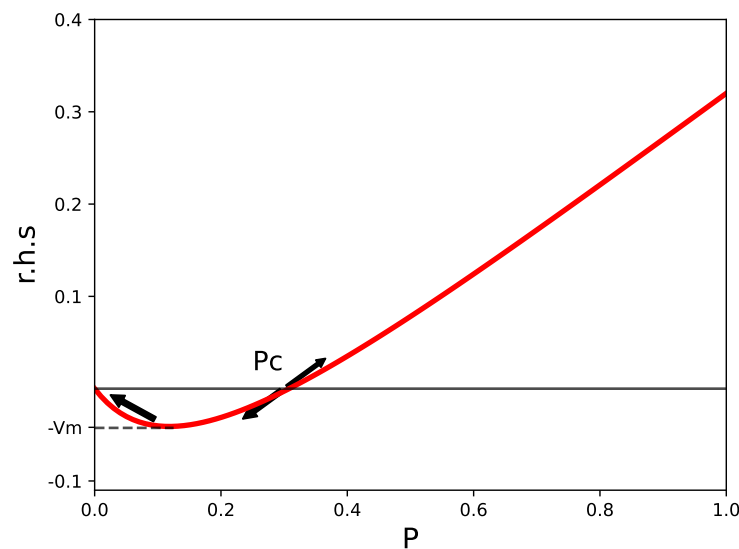


**Figure 1.** The r.h.s. of Equation (2) for  $f_t = 0$ . A stable fixed point at  $P = 0$  and an unstable one at  $P = P_c \approx 0.3$  are signaled. Arrows indicate restoring forces. A third stable critical point at  $P \approx P_s$  corresponds to a septic state, which is not seen in the figure. The value of the function at the minimum,  $-V_m$ , is indicated.

We can roughly estimate  $P_c$  by expanding the r.h.s. of Equation (2) in series of  $P$ , retaining linear and quadratic terms, and equating the result to zero, whereby we obtain

$$P_c = \frac{b_t - a}{b_t c_\infty - a/P_s} \approx \frac{1}{c_\infty}. \tag{3}$$

The last expression comes from neglecting  $a$  against  $b_t$ . We will assume that there is a unique  $c_\infty$  for all of the tissues. This sets a reference value for  $P_c$  in the whole body.  $P_c$  could, probably, be associated with the threshold value for initiating the recruitment of additional immune cells.

#### 2.4. Stability Condition in Tissues

At this point, one may ask the following question: what is the stability condition of the  $P = 0$  healthy state? In other words, how do barriers and the annihilation rate in a given tissue combine in order to guarantee that common pathogen threats are annihilated? The response coefficient  $b_t$ , apart from being greater than  $a$ , shall depend on the pathogen load that the tissue is regularly exposed to. If the flow of pathogens,  $f$ , is practically constant in certain time intervals, one can obtain a stability condition by requiring the r.h.s. of Equation (2) to be lower than zero. This leads to

$$\alpha_t f_t < V_m \approx \frac{b_t}{4c_\infty} \approx \frac{b_t P_c}{4}. \quad (4)$$

$V_m$  is the value at the minimum defined in Figure 1. The estimation for  $V_m$  comes from expanding the r.h.s. in series, in the same way as we did for  $P_c$ . Notice that if the inequality (4) is violated, the r.h.s. of Equation (2) is always greater than zero and  $P$  increases towards  $P_s$ .

Coefficients  $\alpha_t$  and  $b_t$  shall combine in each tissue in order to guarantee that Equation (4) will hold, i.e., guarantee immunity against regular threats. Higher threats (a higher  $f_t$ ) would require higher barriers (a smaller  $\alpha_t$ ) and/or higher annihilation rates ( $b_t$ ). This is typical of epithelial tissues. In other cases, for example, germinal cells in the testis, in order to prevent autoimmunity, the coefficient  $b_t$  is reduced, which is compensated by high barriers. In summary, we may formulate a second explicit statement, suitable also for experimental verification:

**Statement 2.** *The minimization of  $P$  leads to the condition (4) for the coefficients  $\alpha_t$  and  $b_t$  in terms of the regular pathogen flow in the tissue  $f_t$ . An economy of resources implies that the inequality should be near optimal. There is roughly a similar  $P_c$  value in all tissues.*

#### 2.5. A Second Consequence of the Unstable Fixed Point

The unstable fixed point not only sets a unique reference value,  $P_c$ , but is also the reason for an interesting property of the small- $P$  response. When the pathogen load overcomes the stability threshold given by Equation (4), the fixed point slows down the increase in  $P$ . The reason is very simple:  $P$  should traverse the region near  $P_c$ , where the r.h.s. of Equation (2) is near zero; that is, where the net annihilation rate of pathogens surpassing the barrier is close to its effective rate of growth. This is illustrated in Figure 2 for the following particular parameter values:  $V_m \approx 0.04 \text{ h}^{-1}$  and  $\alpha f = 0.05 \text{ h}^{-1}$ . The figure shows that the increase in  $P$  is delayed for more than 20 h, even though the characteristic time scale of the problem is around  $1/b_t$ , which is one hour. This delay allows for the recruitment of immune cells from blood circulation. We may formulate the following:

**Statement 3.** *As a violation of the stability condition, Equation (4) leads to an impasse phase allowing for the recruitment of other immune cells.*

This statement can also be experimentally checked.

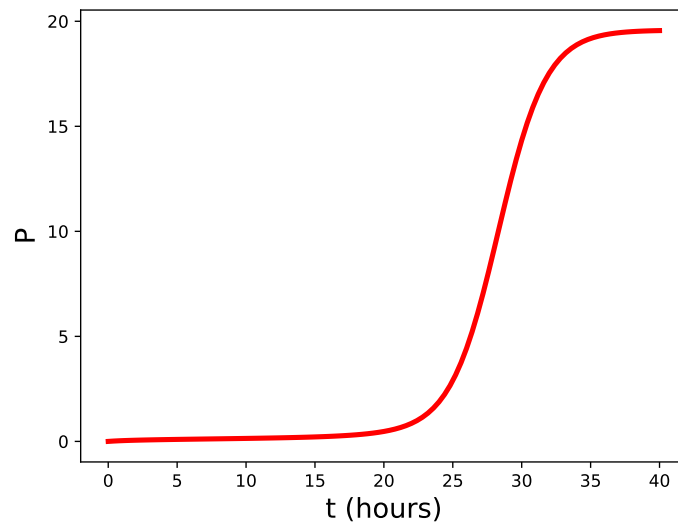


**Figure 2.** Numerical solution of Equation (2) showing the time evolution of  $P$  in the unstable regime characterized by the parameters  $\alpha f = 0.05 \text{ h}^{-1} > Vm = 0.04 \text{ h}^{-1}$ . Notice the 20 h long delay before the increase in  $P$ .

2.6. A Qualitative Comparison

The following example is a qualitative comparison between two nearby tissues: the small and large intestines. An understanding of the reinforced immunity of the small intestine comes from this analysis.

We show in Figure 3 the schematics of the density of microbes in the contact region. These microbes are mainly commensal bacteria, but it is reasonable to assume that the pathogen loads are proportional to these numbers.

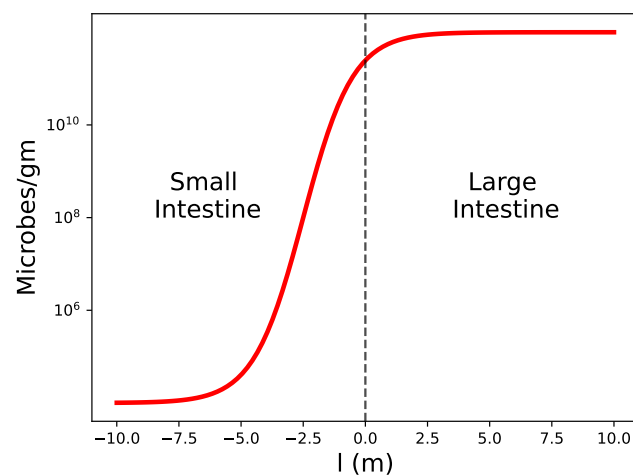


**Figure 3.** Schematic representation of the density of microbes in the gut.

The variable  $l$  is a coordinate along the gut. The small bowel is located at  $l < 0$ , and the large intestine is located at  $l > 0$ . The mean value of the microbes/gm experiences a jump from  $10^4$  to  $10^{11}$  as we cross from the ileum to the cecum [22]. Of course, we expect the dependence to be continuous, as schematically represented in Figure 3.

The parameter values for the large intestine,  $\alpha_l$  and  $b_l$ , are roughly constant. In the small intestine, however, the parameters shall exhibit a spatial variation.  $\alpha_s$  shall decrease and  $b_s$  increase as  $l$  moves towards the distal end of the ileum. Significant variations in the parameters are expected due to the augmented flow of pathogens in many orders of magnitude. This is consistent with the distribution of Paneth cells [23], Peyer’s patches [24], and other structures along the small bowel. Above, we speak about “reinforced” immune

protection in the small intestine, whereby in this sense, the coefficients  $\alpha_s$  and  $b_s$  shall vary in order to increase protection as  $f_t$  increases.

**Statement 4.** *The distribution of immune structures in the small bowel is related to the increasing density of pathogens observed as we cross from the ileum to the cecum.*

2.7. Other Tissues

The stability condition, Equation (4), also allows for the analysis of the tissues in which the flow of pathogens is normal, but  $b_t$  is decreased at the expense of lowering  $\alpha_t$ . These are, for example, the brain [25] and testis [26], where a limit to the cellular immune response is needed for the proper functioning of the tissue. Recall that the values for  $b_t$  can never be lower than  $a$ , as mentioned.

In addition, there are also tissues, like the gallbladder, where the microbicide character of bile [27] could be translated into a lower-than-average  $\alpha_t$  and, possibly, a low  $b_t$ . Notice that we have generalized the meaning of the “barrier” coefficient,  $\alpha_t$ , not limited now to anatomical or mucosal barriers.

In conclusion, we assume that the coefficients  $\alpha_t$  and  $b_t$  take different values for different tissues. The regular flow that the tissue is exposed to,  $f_t$ , basically determines the ratio  $b_t/\alpha_t$ , according to Equation (4). The tissue’s functioning conditions could dictate additional restrictions. For example, in the brain,  $b_t$  should be relatively low to avoid frequent inflammation processes; thus,  $\alpha_t$  should be decreased. This is the origin of the blood–brain barrier.

2.8. Immunity to Cancer

Although the detailed dynamics of cancer onset and development are very complex [28] and partially unknown, one may guess that there should be an inverse correlation between the annihilation rate of pathogens in a tissue,  $b_t$ , and the risk of cancer. Indeed, the cellular immune response is not only responsible for eliminating virus-infected cells, for example, but also dysfunctional and precancerous cells in the tissue. Thus, a low  $b_t$  could be related to a higher-than-normal cancer risk in that tissue. Conversely, one may obtain information for  $b_t$  from the frequency distribution of cancer in the body tissues [17].

It is reasonable to assume that, for the initial stages of tumors in a tissue, an equation similar to Equation (1) holds:

$$\frac{dN}{d\tau} = g_c + a_c N - b_c N, \tag{5}$$

where  $N$  is the (small) number of precancerous cells,  $g_c$  is the rate of creation of such cells in the tissue,  $a_c$  is their division rate, and  $b_c$  is the tissue’s annihilation rate of dysfunctional cells.  $a_c$  can be estimated from the division rate of stem cells in that tissue,  $u_t$ , assuming that cancer cells originate from stem cells [29]. Typically,  $a_c \sim 1/\text{week}$  or even smaller [16]. On the other hand,  $b_c \sim b_t$ , as noticed. Thus,  $b_c \gg a_c$ .

**Statement 5.** *The tissue-annihilation rate of dysfunctional and precancerous cells is similar to the annihilation rate of pathogens because they are both determined by the resident immune cells.*

For  $g_c$ , we may use an equation like  $g_c \sim p N_{sc} u_t$ , where  $N_{sc}$  is the number of stem cells and  $p$  is a probability parameter modeling the carcinogenic effect of both internal processes (free radicals, for example) or external factors (double strand breaks by ionizing radiation, for example).

Equating to zero the r.h.s. of Equation (5) and neglecting  $a_c$  against  $b_c$ , we obtain the average number of precancerous cells in the tissue:

$$N_c \approx g_c/b_c = (p u_t/b_c) N_{sc}. \tag{6}$$

In order to become a true tumor, these cells should pass through a few stages [28] and avoid the adaptive immune system. Nevertheless, it is reasonable to assume that the lifetime risk for cancer in the tissue is proportional to  $N_c$ , that is:

$$\text{risk} \sim (pu_t/b_c)N_{sc}, \tag{7}$$

where we took  $t \approx 80$  years. It is interesting to notice that an expression similar to Equation (7) comes also from a model of oncogenesis in the gene-expression space [17]. We refer to that paper for a more-detailed analysis. For consistency, we reproduce the qualitative inference of  $b_c$  ( $b_t$ ) from the cancer-risk data.

Figure 4 is a replot of the results by Tomasetti and Vogelstein [16] (see also [30]) showing the dependence of the lifetime risk for cancer in a tissue on the number of stem cells and the rate of mitotic divisions. The  $y$ -axis in the figure is the normalized risk, i.e., the risk per stem cell. This normalization allows for a comparison between tissues with high differences in the number of stem cells. The  $x$ -axis, on the other hand, counts the number of stem cell generations along a lifetime,  $N_{gen}$ , a number roughly proportional to the division rate,  $N_{gen} \approx u_t \cdot 80 \text{ years} + \log_2 N_{sc}$ . The last term accounts for divisions along the clonal expansion phase during tissue formation. The figure shows that, for a single-cell lineage, the larger  $N_{gen}$ , the higher the normalized risk also.

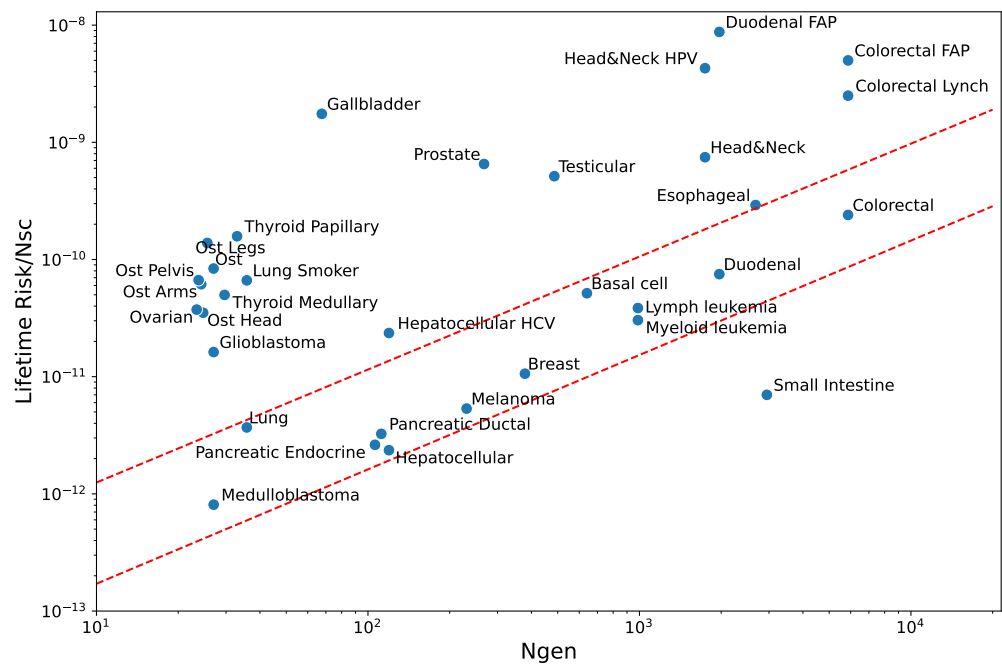


**Figure 4.** Lifetime cancer risk per stem cell vs. the number of stem cell generations in tissues. The figure is a replot of the data contained in Tomasetti and Vogelstein paper [16].

In Figure 4, a set of 11 cancers shows a near-perfect linear correlation:  $\text{risk}/N_{sc} \sim N_{gen}$ , where the proportionality coefficient may be roughly written as  $qp/b_t/80 \text{ years}$ , and  $q$  measures the success rate of precancerous cells: one in ten thousand cells becomes a tumor, for example.

We shall qualify these tissues as “normal”. For all of them, we expect a very similar  $p$  and  $b_t$ , although they may exhibit very different barriers ( $\alpha_t$ ). Indeed, we expect a very low  $\alpha_t$  in the colon and skin but  $\alpha_t \approx 1$  in blood, for example. The only “special” case in this group is the cerebellum, with a high barrier and a normal (instead of a low)  $b_t$ . This means a possibility higher than that in the cerebrum to clear any infection [31].

External and genetic factors raise the risk (through  $p$ ) many times, as compared to normal tissues. For example, smoking multiplies the risk for lung cancer by roughly 20 and, in familial adenomatous polyposis patients, the risk for colon cancer is increased by a factor around 100.

There are also tissues like the brain, germ cells, gallbladder, bones, and thyroid where, in addition to genetic or external factors, the relatively high normalized values for the risk lead one to suspect unusually low values of  $b_t$ . The brain, germ cells, and the gallbladder were briefly discussed above. About bones, it is known that immunity relies strongly on defensins [32], possibly with a relatively low number of resident cells. On the other hand, the thyroid is known to have a close cross-talk with the immune system [33]. Its dysregulation is the cause of immune disorders. One may speculate that a low number of resident cells is needed to prevent autoimmunity in the thyroid.

Finally, we have the small intestine with a normalized risk lower than normal, possibly related to a high average  $b_t$ , a fact consistent with what was discussed above. The results for the estimated coefficients are summarized in Table 1. Although these are only qualitative results, they allow for a comparison between tissues and are a first step towards the understanding of Figure 4 for the lifetime risks of cancer in different tissues. We may formulate the following:

**Statement 6.** *The characteristics of the immune system for a set of tissues are qualitatively described in Table 1. The cancer risk shows an inverse correlation with the cellular immune response against infections.*

**Table 1.** Qualitative comparison of immunity in tissues. The cancer risk per stem cell assumes no external carcinogens or genetic predisposition.

Tissue	Pathogen Flow ( $f_t$ )	Barrier Height ( $1/\alpha_t$ )	Annihilation Rate ( $b_t$ )	Cancer Risk
Small bowel	Very High	High	High	Low
Colon	Very High	Very High	Normal	Normal
Lung	Very High	Very High	Normal	Normal
Skin	Very High	Very High	Normal	Normal
Duodenum	High	High	Normal	Normal
Blood	Normal	Normal	Normal	Normal
Pancreas	Normal	Normal	Normal	Normal
Liver	High	High	Normal	Normal
Cerebellum	Normal	High	Normal	Normal
Esophagus	High	High	Normal	Normal
Head and Neck	Normal	Normal	Normal	Normal
Germ cells	Normal	High	Low	High
Brain	Normal	High	Low	High
Gallbladder	Normal	High	Low	High
Bone	Normal	High	Low	High
Thyroid	Normal	High	Low	High

### 3. Discussion

In this paper, we show that simple mathematical ideas lead to interesting results when applied to the innate immune system.

In the simplest linear approximation, Equation (1), the stability of a tissue against small threats requires the annihilation rate to be greater than the average replication rate of pathogens.

The linear model is modified, Equation (2), in order to take into account that neither the number of pathogens nor the response can grow without limits. Healthy ( $P = 0$ ) and septic ( $P = P_s$ ) states appear as fixed points of the nonlinear (self-regulated) equation. In the middle of the way, an additional unstable fixed point,  $P = P_c$ , signals the transition

from healthy to septic regimes. We postulate that the value of  $P_c$  is common to all tissues. The tissue is in a stable healthy condition if the inequality given in Equation (4) is fulfilled. In other words, the barrier and the cellular component of the immunity are adjusted to the regular flow of pathogens in the tissue. In the colon, for example, characterized by a very high density of pathogens, we expect high barriers and a normal annihilation rate.

We noticed that the distribution frequency of cancer in tissues provides indications about the strength of the annihilation rate of pathogens, under the assumption that it is correlated with the rate of annihilation of precancerous cells. This later assumption follows from the fact that both  $b_c$  and  $b_t$  are determined by the resident immune cells in the tissue. Thus, the observation of a high cancer risk per stem cell in the gallbladder, for example, indicates a low annihilation rate of pathogens by the immune cells, and this is consistent with the fact that bile provides an effective barrier against bacteria.

The main results of this paper allow for a comparison of the immune response in different tissues and establish a relation between immunity to infections and to cancer. Table 1 offers a kind of summary. To the best of our knowledge, there are no similar results in the literature. In this paper, we formulate them in the form of precise statements, with the hope that they could be quantitatively checked by using present-day immunology techniques.

There are many possible future directions of work. For example, to uncover the dependence of  $b_t$  on the total number of cells in a tissue,  $N_{cell}$  can be used. As  $b_t$  is mainly the result of the resident immune cells, it is natural to expect that a larger tissue would require more resident cells in order to guarantee immunity. Almost naive arguments lead to the estimation  $N_{cell}^\beta$  for the number of resident cells [34], where the power beta is around 2/3. The power dependence is consistent with the scaling hypothesis in biology [35,36]. We performed a rough checking of this law for tissue resident macrophages in mice, which leads to a  $\beta$  of nearly one. The number of macrophages in different tissues is indirectly obtained by measuring the level of a macrophage-specific antibody, F4/80 [37]. This direction of work deserves further attention.

However, what we like most is the perspective of looking at the immune ecosystem formed by tissues and the body microbiota [38]. Equilibrium in this ecosystem is synonymous of a healthy state. Dysregulations or disequilibrium, on the other hand, are indications of diseases. Work along some of these directions is in progress.

**Author Contributions:** Conceptualization, A.G.; methodology, R.H., J.N. and A.G.; software, R.H. and J.N.; investigation, R.H., J.N. and A.G.; writing—original draft preparation, A.G.; writing—review and editing, R.H., J.N. and A.G. All authors have read and agreed to the published version of the manuscript.

**Funding:** This research received no external funding.

**Institutional Review Board Statement:** Each author declares that this article does not contain any studies with animals performed by any of the authors.

**Informed Consent Statement:** This is to declare that the research reported herein does not involve human participants and/or animals.

**Data Availability Statement:** The data for Figure 4 are available in the supplementary materials of Ref. [16]. The code used to generate the figures is available at the GitHub repository <https://github.com/RobertoHePe/F-S-Dynamics> accessed on 26 September 2023.

**Acknowledgments:** The authors acknowledge the Cuban Agency for Nuclear Energy and Advanced Technologies (AENTA) and the Office of External Activities of the Abdus Salam Centre for Theoretical Physics (ICTP) for their support.

**Conflicts of Interest:** The authors declare no conflict of interest.

## References

1. Murphy, K.; Weaver, C. *Janeway's Immunobiology*; Garland Science: New York, NY, USA, 2016.
2. Akira, S.; Uematsu, S.; Takeuchi, O. Pathogen recognition and innate immunity. *Cell* **2006**, *124*, 783–801. [[CrossRef](#)] [[PubMed](#)]
3. Demaria, O.; Cornen, S.; Daëron, M.; Morel, Y.; Medzhitov, R.; Vivier, E. Harnessing innate immunity in cancer therapy. *Nature* **2019**, *574*, 45–56. [[CrossRef](#)]

4. Eftimie, R.; Gillard, J.J.; Cantrell, D.A. Mathematical models for immunology: Current state of the art and future research directions. *Bull. Math. Biol.* **2016**, *78*, 2091–2134. [[CrossRef](#)]
5. Davis, M.M.; Tato, C.M.; Furman, D. Systems immunology: Just getting started. *Nat. Immunol.* **2017**, *18*, 725–732. [[CrossRef](#)]
6. Vlazaki, M.; Huber, J.; Restif, O. Integrating mathematical models with experimental data to investigate the within-host dynamics of bacterial infections. *Pathog. Dis.* **2019**, *77*, ftaa001. [[CrossRef](#)]
7. Xavier, J.B.; Monk, J.M.; Poudel, S.; Norsigian, C.J.; Sastry, A.V.; Liao, C.; Bento, J.; Suchard, M.A.; Arrieta-Ortiz, M.L.; Peterson, E.J.R.; et al. Mathematical models to study the biology of pathogens and the infectious diseases they cause. *iScience* **2022**, *25*, 104079. [[CrossRef](#)] [[PubMed](#)]
8. Van Dyke, T.; Jacks, T. Cancer modeling in the modern era: Progress and challenges. *Cell* **2002**, *108*, 135–144. [[CrossRef](#)]
9. Quaranta, V.; Weaver, A.M.; Cummings, P.T.; Anderson, A.R. Mathematical modeling of cancer: The future of prognosis and treatment. *Clin. Chim. Acta* **2005**, *357*, 173–179. [[CrossRef](#)]
10. Altrock, P.M.; Liu, L.L.; Michor, F. The mathematics of cancer: Integrating quantitative models. *Nat. Rev. Cancer* **2015**, *15*, 730–745. [[CrossRef](#)]
11. Tabassum, S.; Rosli, N.B.; Binti Mazalan, M.S.A. Mathematical modeling of cancer growth process: A review. *J. Phys. Conf. Ser.* **2019**, *1366*, 012018. [[CrossRef](#)]
12. Mohler, R.R.; Lee, K.S.; Asachenkov, A.L.; Marchuk, G.I. A systems approach to immunology and cancer. *IEEE Trans. Syst. Man Cybern.* **1994**, *24*, 632–642. [[CrossRef](#)]
13. Marchuk, G.I. *Mathematical Modelling of Immune Response in Infectious Diseases*; Springer Science & Business Media: New York, NY, USA, 1997; Volume 395.
14. Foryś, U. Marchuk’s model of immune system dynamics with application to tumour growth. *J. Theor. Med.* **2002**, *4*, 85–93. [[CrossRef](#)]
15. Su, B.; Zhou, W.; Dorman, K.; Jones, D. Mathematical modelling of immune response in tissues. *Comput. Math. Methods Med.* **2009**, *10*, 9–38. [[CrossRef](#)]
16. Tomasetti, C.; Vogelstein, B. Variation in cancer risk among tissues can be explained by the number of stem cell divisions. *Science* **2015**, *347*, 78–81. [[CrossRef](#)] [[PubMed](#)]
17. Herrero, R.; Leon, D.A.; Gonzalez, A. A one-dimensional parameter-free model for carcinogenesis in gene expression space. *Sci. Rep.* **2022**, *12*, 4748. [[CrossRef](#)] [[PubMed](#)]
18. Davies, L.C.; Jenkins, S.J.; Allen, J.E.; Taylor, P.R. Tissue-resident macrophages. *Nat. Immunol.* **2013**, *14*, 986–995. [[CrossRef](#)]
19. Beckers, H.; Van der Hoeven, J. Growth rates of *Actinomyces viscosus* and *Streptococcus mutans* during early colonization of tooth surfaces in gnotobiotic rats. *Infect. Immun.* **1982**, *35*, 583–587. [[CrossRef](#)]
20. Mai, M.; Wang, K.; Huber, G.; Kirby, M.; Shattuck, M.D.; O’Hern, C.S. Outcome prediction in mathematical models of immune response to infection. *PLoS ONE* **2015**, *10*, e0135861. [[CrossRef](#)] [[PubMed](#)]
21. Nemytskii, V.V. *Qualitative Theory of Differential Equations*; Princeton University Press: Princeton, NJ, USA, 2015; Volume 2083.
22. O’Hara, A.M.; Shanahan, F. The gut flora as a forgotten organ. *EMBO Rep.* **2006**, *7*, 688–693. [[CrossRef](#)]
23. Clevers, H.C.; Bevins, C.L. Paneth cells: Maestros of the small intestinal crypts. *Annu. Rev. Physiol.* **2013**, *75*, 289–311. [[CrossRef](#)]
24. Jung, C.; Hugot, J.P.; Barreau, F. Peyer’s patches: The immune sensors of the intestine. *Int. J. Inflamm.* **2010**, *2010*, 823710. [[CrossRef](#)]
25. Van Sorge, N.M.; Doran, K.S. Defense at the border: The blood–brain barrier versus bacterial foreigners. *Future Microbiol.* **2012**, *7*, 383–394. [[CrossRef](#)]
26. França, L.R.; Auharek, S.A.; Hess, R.A.; Dufour, J.M.; Hinton, B.T. Blood-tissue barriers: morphofunctional and immunological aspects of the blood-testis and blood-epididymal barriers. In *Biology and Regulation of Blood-Tissue Barriers*; Springer: Berlin/Heidelberg, Germany, 2013; pp. 237–259.
27. Merritt, M.E.; Donaldson, J.R. Effect of bile salts on the DNA and membrane integrity of enteric bacteria. *J. Med. Microbiol.* **2009**, *58*, 1533–1541. [[CrossRef](#)]
28. Frank, S.A. *Dynamics of Cancer: Incidence, Inheritance, and Evolution*; Princeton University Press: Princeton, NJ, USA, 2007.
29. Reya, T.; Morrison, S.J.; Clarke, M.F.; Weissman, I.L. Stem cells, cancer, and cancer stem cells. *Nature* **2001**, *414*, 105–111. [[CrossRef](#)]
30. Wu, S.; Powers, S.; Zhu, W.; Hannun, Y.A. Substantial contribution of extrinsic risk factors to cancer development. *Nature* **2016**, *529*, 43–47. [[CrossRef](#)] [[PubMed](#)]
31. Hooper, D.C.; Phares, T.W.; Kean, R.B.; Mikheeva, T. Regional Differences in Blood-Brain Barrier. *J. Immunol.* **2006**, *176*, 7666–7675.
32. Varoga, D.; Wruck, C.; Tohidnezhad, M.; Brandenburg, L.; Paulsen, F.; Mentlein, R.; Seekamp, A.; Besch, L.; Pufe, T. Osteoblasts participate in the innate immunity of the bone by producing human beta defensin-3. *Histochem. Cell Biol.* **2009**, *131*, 207–218. [[CrossRef](#)] [[PubMed](#)]
33. Perrotta, C.; De Palma, C.; Clementi, E.; Cervia, D. Hormones and immunity in cancer: Are thyroid hormones endocrine players in the microglia/glioma cross-talk? *Front. Cell. Neurosci.* **2015**, *9*, 236. [[CrossRef](#)] [[PubMed](#)]
34. Gonzalez, A. Estimating the number of tissue resident macrophages. *arXiv* **2016**, arXiv:1603.08397.
35. West, G.B.; Brown, J.H.; Enquist, B.J. A general model for the origin of allometric scaling laws in biology. *Science* **1997**, *276*, 122–126. [[CrossRef](#)]
36. Savage, V.M.; Gillooly, J.F.; Woodruff, W.H.; West, G.B.; Allen, A.P.; Enquist, B.J.; Brown, J.H. The predominance of quarter-power scaling in biology. *Funct. Ecol.* **2004**, *18*, 257–282. [[CrossRef](#)]

37. Lee, S.H.; Starkey, P.M.; Gordon, S. Quantitative analysis of total macrophage content in adult mouse tissues. Immunochemical studies with monoclonal antibody F4/80. *J. Exp. Med.* **1985**, *161*, 475–489. [[CrossRef](#)] [[PubMed](#)]
38. Hou, K.; Wu, Z.X.; Chen, X.Y.; Wang, J.Q.; Zhang, D.; Xiao, C.; Zhu, D.; Koya, J.B.; Wei, L.; Li, J.; et al. Microbiota in health and diseases. *Signal Transduct. Target. Ther.* **2022**, *7*, 135. [[CrossRef](#)] [[PubMed](#)]

**Disclaimer/Publisher's Note:** The statements, opinions and data contained in all publications are solely those of the individual author(s) and contributor(s) and not of MDPI and/or the editor(s). MDPI and/or the editor(s) disclaim responsibility for any injury to people or property resulting from any ideas, methods, instructions or products referred to in the content.